Food Chemistry 119 (2010) 286–297

Contents lists available at ScienceDirect

Food Chemistry

journal homepage: www.elsevier.com/locate/foodchem

Controlling fat bloom formation in chocolate – Impact of milk fat on microstructure and fat phase crystallisation

Sopark Sonwai [a], Dérick Rousseau [b,*]

[a] Department of Food Technology, Faculty of Engineering and Industrial Technology, Silpakorn University, Nakornpathom 73000, Thailand
[b] Department of Chemistry and Biology, Ryerson University, Toronto, Ontario, Canada M5B 2K3

ARTICLE INFO

Article history:
Received 12 December 2008
Received in revised form 12 June 2009
Accepted 16 June 2009

Keywords:
Chocolate
Fat bloom
Atomic force microscopy
Microstructure
Crystallisation
Milk fat

ABSTRACT

The partial replacement of cocoa butter (CB) with milk fat (MF) strongly influences micro-scale topographic evolution and fat phase crystallisation in milk chocolate. Adding MF reduces the incidence of large surface crystals and the number and diameter of amorphous, welled CB deposits ('cones'), with a concurrent decrease in initial surface roughness ($p < 0.05$) and rate of surface coarsening. Presence of MF also slows the solidification of the cones into disorganised crystalline masses. Finally, MF reduces the initial solid fat content, and slows the rate of change in whiteness index, as well as the form V to VI polymorphic transition. Fat crystal growth is accelerated by repeated temperature-cycling (26–29 °C) compared to isothermal conditioning (26 °C). However, cone hardening occurs more rapidly when isothermally-stored. Irrespective of fat composition and storage conditions, fat crystal growth, welling and ultimately fat bloom begin only at specific locations on the chocolate surface, suggesting that chocolate's microstructural heterogeneity is responsible for distinct surface fat crystallisation pathways.

1. Introduction

Industrial milk chocolate is manufactured using well-established protocols that result in a product with defined organoleptic attributes. From a colloidal perspective, chocolate consists of micron-scale particulates (sugar crystals, cocoa particles, and milk powder) dispersed within a solid/liquid fat phase consisting primarily of cocoa butter (CB). The CB, which is made up of 3 key triglycerides (TGs) [1,3-dipalmitoyl-2-oleoyl-glycerol (POP), 1,3-distearoyl-2-oleoyl-glycerol (SOS) and *rac*-palmitoyl-stearoyl-2-oleoyl-glycerol (POS)], is polymorphic, with six known forms, identified with either Greek nomenclature (γ, α, β_2', β_1', β_2 and β_1) or Roman numerals (forms I through VI), in ascending stability (Loisel, Keller, Lecq, Bourgaux, & Ollivon, 1998). All cocoa butter polymorphic transitions are monotropic and take place *via* either a solid-state transition or by melt-mediation. Industrially, crystallisation of the form β_2 (form V) polymorph is promoted as it confers chocolate products proper snap (ability to break apart easily), good demoulding properties (contraction) and a good quality finish in terms of colour and gloss. As the chocolate is processed, dynamic phenomena that take place in (and on) chocolate within short timescales (minutes to hours), such as micro-scale ordering and association of the dispersed particulate, as well as triglyceride (TG) nucleation and growth, directly impact longer-timescale quality attributes, such as texture and bloom appearance (Rousseau & Smith, 2008; Rousseau & Sonwai, 2008).

The primary source of fat bloom is generally thought to result from the growth of pre-existing fat crystals at the surface of chocolate (Aguilera, Michel, & Mayor, 2004; Jewell, 1972; Lonchampt & Hartel, 2004; Timms, 1984; Vaeck, 1960). However, it is not exactly known how these crystals grow, and why fat bloom initially occurs only at specific locations on the surface. Previous efforts from our group have shown that fat bloom crystals arise from two sources: (i) pre-existing surface crystals that act as templates for larger bloom-causing crystals, and (ii) amorphous, welled regions ('cones') that solidify with age and act as loci for subsequent crystal outcrops (Sonwai & Rousseau, 2008).

As the fat phase clearly has a bearing on the sensory attributes of chocolate, it is imperative to determine CB's crystallisation behaviour and the close link with composition. Partial replacement of CB with milkfat (MF) in chocolate formulations is now a common industrial practice as it improves bloom resistance and appreciably softens texture (Lonchampt & Hartel, 2004) by lowering the initial solid fat content, by slowing down the rate of CB crystallisation (Timms, 2003) and by retarding the form V → VI transition, as MF is β'-stable (Lohman & Hartel, 1994). Here, we provide a detailed analysis of the influence of MF on micro-scale topographic evolution and bloom development in chocolate, using chocolates

* Corresponding author. Address: Department of Chemistry and Biology, Ryerson University, 350 Victoria Street, Toronto, Ontario, Canada M5B 2K3 Tel.: +1 416 979 5000x2155; fax: +1 416 979 5044.
E-mail addresses: rousseau@ryerson.ca, ssonwai@gmail.com (D. Rousseau).

0308-8146/$ - see front matter © 2009 Elsevier Ltd. All rights reserved.
doi:10.1016/j.foodchem.2009.06.031

made with different proportions of MF. The key outcome is a better understanding of the structural evolution in chocolate over time.

2. Materials and methods

Four milk chocolate formulations with differing amounts of MF were manufactured by Cadbury Canada (Toronto, Canada). CB (32% w/w) was replaced with either 2.5% (chocolate #2), 5% (chocolate #3) or 7.5% MF (w/w) (chocolate #4), and compared to the control, which consisted solely of CB (chocolate #1). The chocolates were tempered in a lab-scale temperer before being poured into plastic moulds and solidified into thin chocolate bars (0.4 cm × 3 cm × 12 cm). The MF (99.7% purity), was purchased from Parmalat (Toronto, Canada). Once removed from the moulds, each chocolate bar was packaged in a plastic bag and sealed. About 50 bars were made for each formulation. The samples were then put inside a Styrofoam box and transported to Ryerson University (a 15-min trip), where they were transferred to a temperature-controlled cabinet set at 26 ± 0.5 °C. To rapidly discern the effects of added MF, repeated temperature-cycling, from 26 to 29 °C, was used to accelerate the structural changes in the chocolates. After an initial 12 h period at 26 °C, the samples were transferred to a 2nd temperature-controlled cabinet set at 29 ± 0.5 °C for 12 h and then put back into the first cabinet. This procedure was repeated every 12 h for 4 weeks, during which their properties were monitored weekly. Sample characterisation at week 0 was performed after the samples had been kept at 26 °C for 1 h. The control chocolate was also held isothermally for 4 weeks at 26 ± 0.5 °C, so as to further discern the impact of temperature-cycling. Ten bars per formulation were required for each set of analyses: 2 for X-ray diffraction (XRD), 3 for colour measurements, 3 for solid fat content (SFC) determinations and 2 for atomic force microscopy (AFM) assessment. Characterisation was performed at 26 °C and all samples were sacrificed following analysis.

A Bioscope AFM with Nanoscope IIIa controller (Digital Instruments, Santa Barbara, CA, USA), operated in 'tapping' mode, was used to image the surface of the moulded side of the chocolate bars. The AFM tips had a cantilever spring constant of 40 N/m and were oscillated at ~350 kHz with an end-point radius of 10 nm and a body angle of 30°. Height, amplitude and phase imaging of regions ranging from 25 μm × 25 μm to 5 μm × 5 μm were recorded. Height and amplitude data provided information on the microtopography of the chocolates whereas phase imaging was used to gain qualitative insights regarding surface microrheology. All images were highly representative of the chocolate surface at a given storage time. Images were processed post-capture, using Gwyddion v2.10 (Czech Metrology Institute, Czech Republic). The root mean square (RMS) surface roughness of all chocolates was also determined, and is based on the height deviations taken from the mean data plane:

$$\mathrm{RMS} = \sqrt{\frac{1}{N}\sum_{i=1}^{N} Z_i^2} \quad (1)$$

where Z and N are the individual height deviations from the mean data plane and the number of measurements, respectively. The same scan size (25 μm × 25 μm) was used for all roughness evaluations, which permitted adequate sampling and allowed for direct comparison of important surface features. XRD, SFC measurements and whiteness index (WI) analyses were performed as previously described (Sonwai & Rousseau, 2008). Quantification of forms V and VI in the XRD spectra was performed as in a previous protocol (Sonwai & Rousseau, 2006).

3. Results and discussion

3.1. Fresh chocolate topography

The surface of freshly-tempered chocolates #1 through #4 (Figs. 1–4) was smooth with limited mottling and few surface imperfections, when viewed at a 25 × 25 μm scan size (Figs. 1a and b, 2a and b, 3a and b and 4a and b). Close-up scans of the 4 chocolates (Figs. 1c, 2c, 3c, 4c) revealed the presence of surface fat crystal platelets <5 μm in length (white arrows in Figs. 1c, 2c and 3c). Based on their size, these crystals confirmed that the chocolates had been correctly tempered with their fat phase existing in the form V polymorph. Small, amorphous cone-like drops were also scattered on the surface of all chocolates, with many showing irregular shapes, pitting and collapsed sides, particularly in the control chocolate (black arrows in Fig. 1c). The initial surface cone concentration, defined as the average number of cones per five 25 μm × 25 μm areas, was 7.7 ± 0.9, 4.3 ± 0.5, 2.3 ± 0.5 and 1.3 ± 0.3 for chocolates #1–#4, respectively ($p < 0.05$). At week 0, cones measured ~2 μm in diameter on the CB-only chocolate whereas, on chocolate #4, they averaged well below 1 μm.

3.2. Evolution in topography during storage

Chocolate ageing was dominated by increases in surface roughness, crystal size and cone diameter, along with notable changes in cone morphology. After 1 week, cones on chocolate #1 grew in size, but maintained their fairly smooth texture (Fig. 1d–f), whereas the surrounding surface displayed extensive crystal growth. Also visible were surface depressions ~1 μm in depth (black arrows in Fig. 1f), likely formed during post-temper cooling and crystallisation. At 2 weeks (Fig. 1g–i), the rate of increase in cone number slowed whereas surface crystallisation continued. Significantly, many crystals formed in the vicinity of the cones, and this continued at 3 weeks (Fig. 1j–l). At 4 weeks (Fig. 1m–o), needles up to ~8 μm in length were present and the cone surfaces were beginning to roughen. The average cone diameter on chocolate #1 increased from 1.9 ± 0.2 μm to 9.4 ± 0.1 μm, in a linear fashion ($r^2 = 0.97$), at a rate of ~1.9 μm/week ($p < 0.05$).

Microstructural evolution of chocolate #2 was phenomenologically similar to that of chocolate #1 (Fig. 2), with the added MF slowing both cone formation and background surface crystallisation. At 1 week (Fig. 2d–f), cones increased in both size and number, though at a much slower rate than on chocolate #1. Protruding crystals began appearing at 2 weeks (Fig. 2g–i), a delay of 1 week compared to chocolate #1. At 3 and 4 weeks of storage (Fig. 2j–l and 2m–o), there were no further changes in either cone number or size. However, surface crystal growth continued, with some crystalline ridges >25 μm in length visible (Fig. 2j and k). After 4 weeks, the majority of the cones remained smooth, indicating that the addition of 2.5% MF strongly altered fat phase crystallisation kinetics, particularly with temperature-cycling. These results were somewhat counter-intuitive as the MF was expected to evenly delay surface crystal growth across the entire surface. Instead, only cone-associated crystallisation was delayed whereas surface crystal growth appeared to be promoted by the MF, once it actually began. These findings suggested that the addition of MF to the fat phase, below an optimal concentration, sufficiently increased CB TG mobility to promote surface crystal growth, perhaps as a result of CB TG fractionation into lower and higher-melting TGs. These results also supported the notion of compositional heterogeneity playing a role in fat phase microstructural evolution, with the welled regions consisting of lower-melting TGs and the 'structuring' TGs (those in the 'body' of the chocolate) consisting of their higher-melting counterparts. The consequence of such

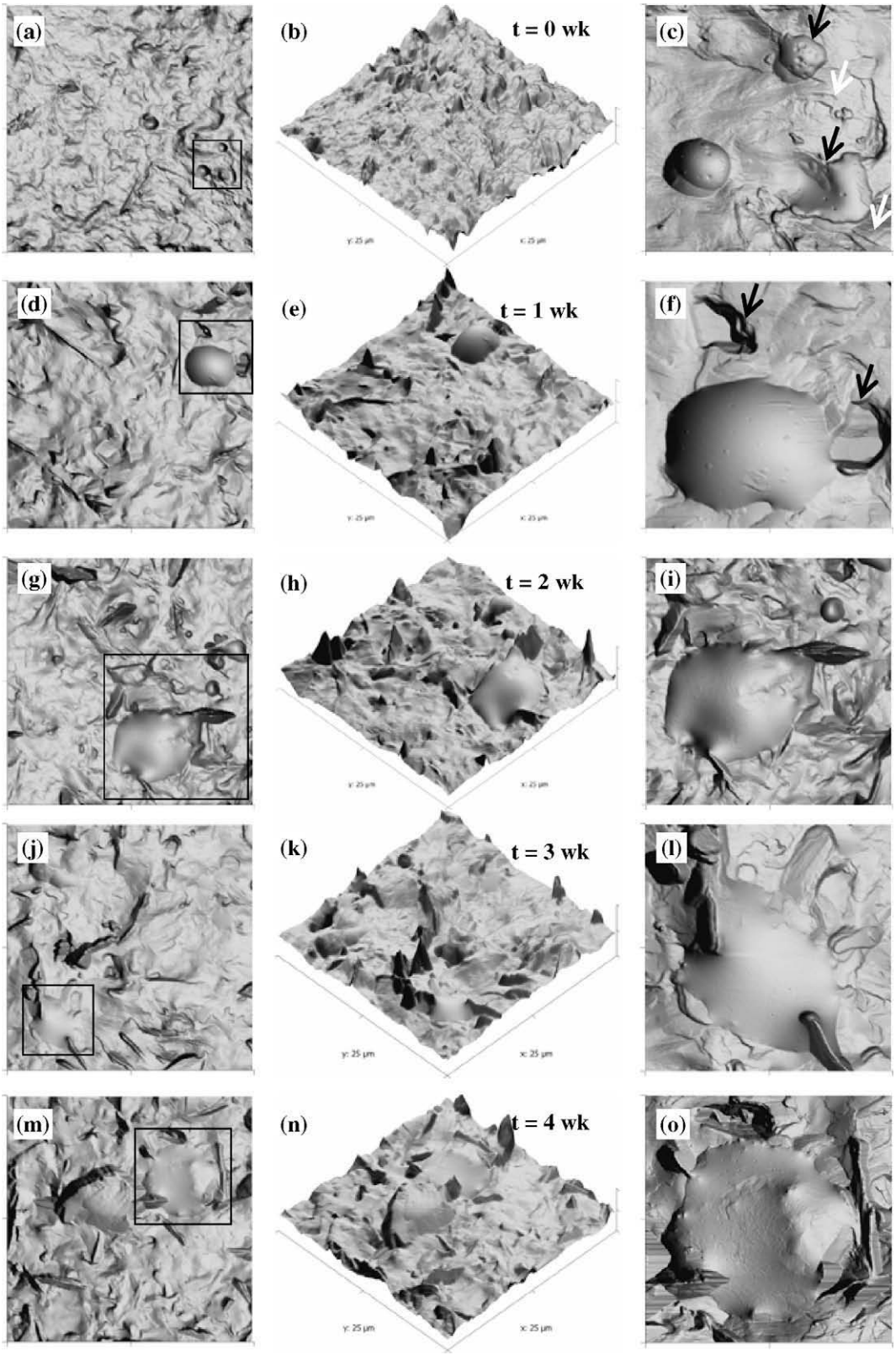

Fig. 1. AFM scans of chocolate #1 repeatedly cycled from 26 to 29 °C over 4 weeks. The left-hand column represents 2-D scans with the corresponding 3-D projections shown in the middle column (25 × 25 μm). The scans in the right-hand column are close-up scans of the area identified by the square boxes in the 25 × 25 μm scans (5 × 5 μm for (c), 8 × 8 μm for (f), 15 × 15 μm for (i), 7.5 × 7.5 μm for (l) and 10 × 10 μm for (o)). The *z*-axis scale (2 μm per division) is accentuated to better depict areas of interest.

compositional variety was that some regions were more susceptible to uncontrolled crystal growth than were others.

The formation and growth of surface fat crystals and the amorphous welled regions were substantially reduced with the addition of 5% and 7.5% MF. On chocolate #3, cones were visible from week 0 (Fig. 3a–c); however, these were very small, and of little consequence to the microstructural development of the chocolate. The surface after 1 week (Fig. 3d–f) was indistinguish-

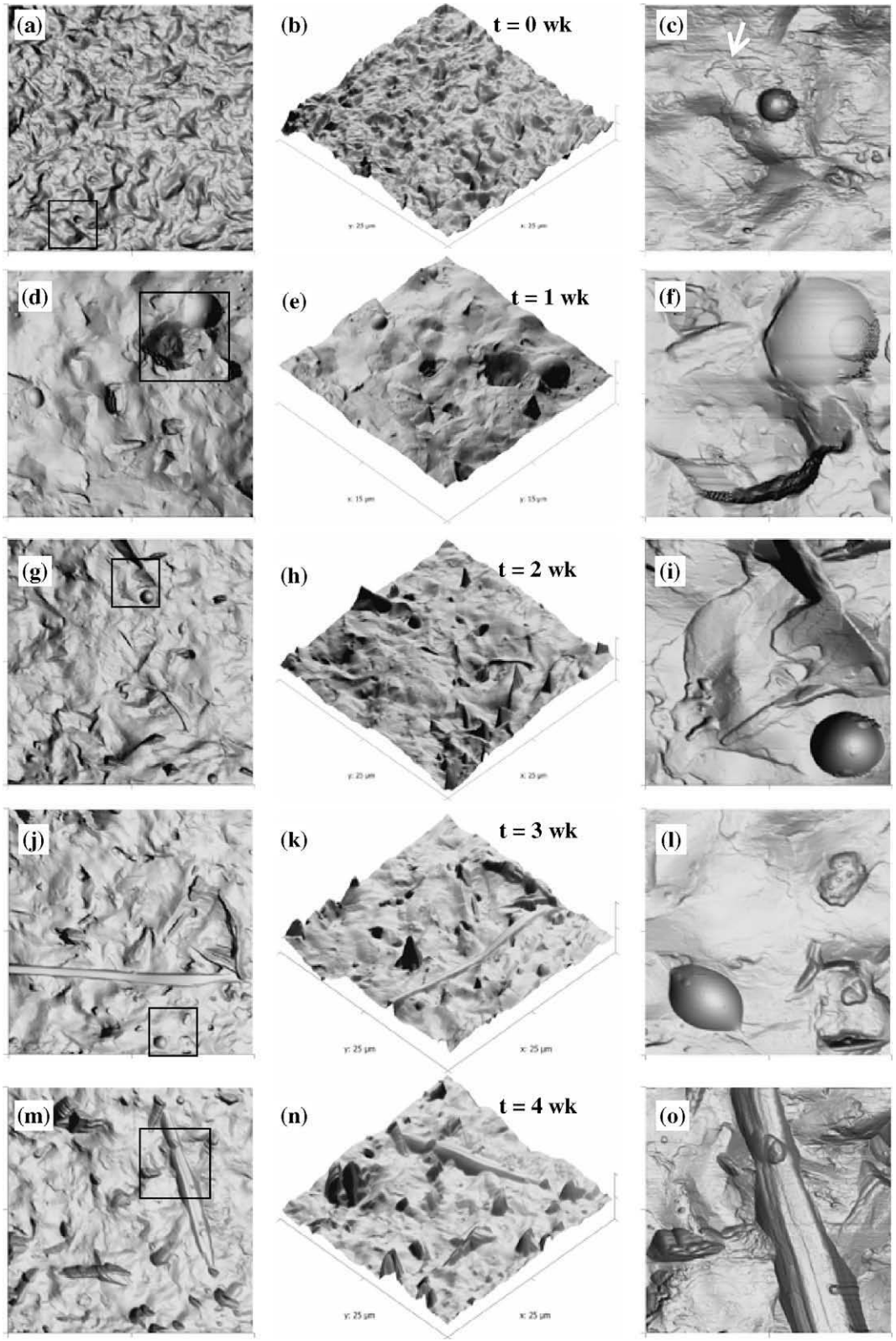

Fig. 2. AFM scans of chocolate #2 repeatedly cycled from 26 to 29 °C over 4 weeks. The left-hand column represents 2-D scans with the corresponding 3-D projections shown in the middle column (25 × 25 μm for (a and b), (g and h), (j and k) and (m and n) and 15 × 15 μm for (d and e)). The scans in the right-hand column are close-up scans of the area identified by the square boxes in the left-hand column (5 × 5 μm for (c), (f), (i), (l) and 7.5 × 7.5 μm for (o)). The *z*-axis scale (2 μm per division) is accentuated to better depict areas of interest.

able from that at week 0 whereas, after 2 weeks (Fig. 3g–i) and 3 weeks (Fig. 3j–l), there was some small-scale surface growth. Some protruding surface crystals appeared at 4 weeks (Fig. 3m and n). Chocolate #4 was virtually free of large surface crystals and cones over the entire storage period. Its surface, after 1 week (Fig. 4d–f) and 2 weeks (Fig. 4g–i) was similar to that of week 0. Some surface crystal growth was evident at 3 weeks (Fig. 4j–l) and 4 weeks (Fig. 4m and n). Overall, chocolates #3 and #4

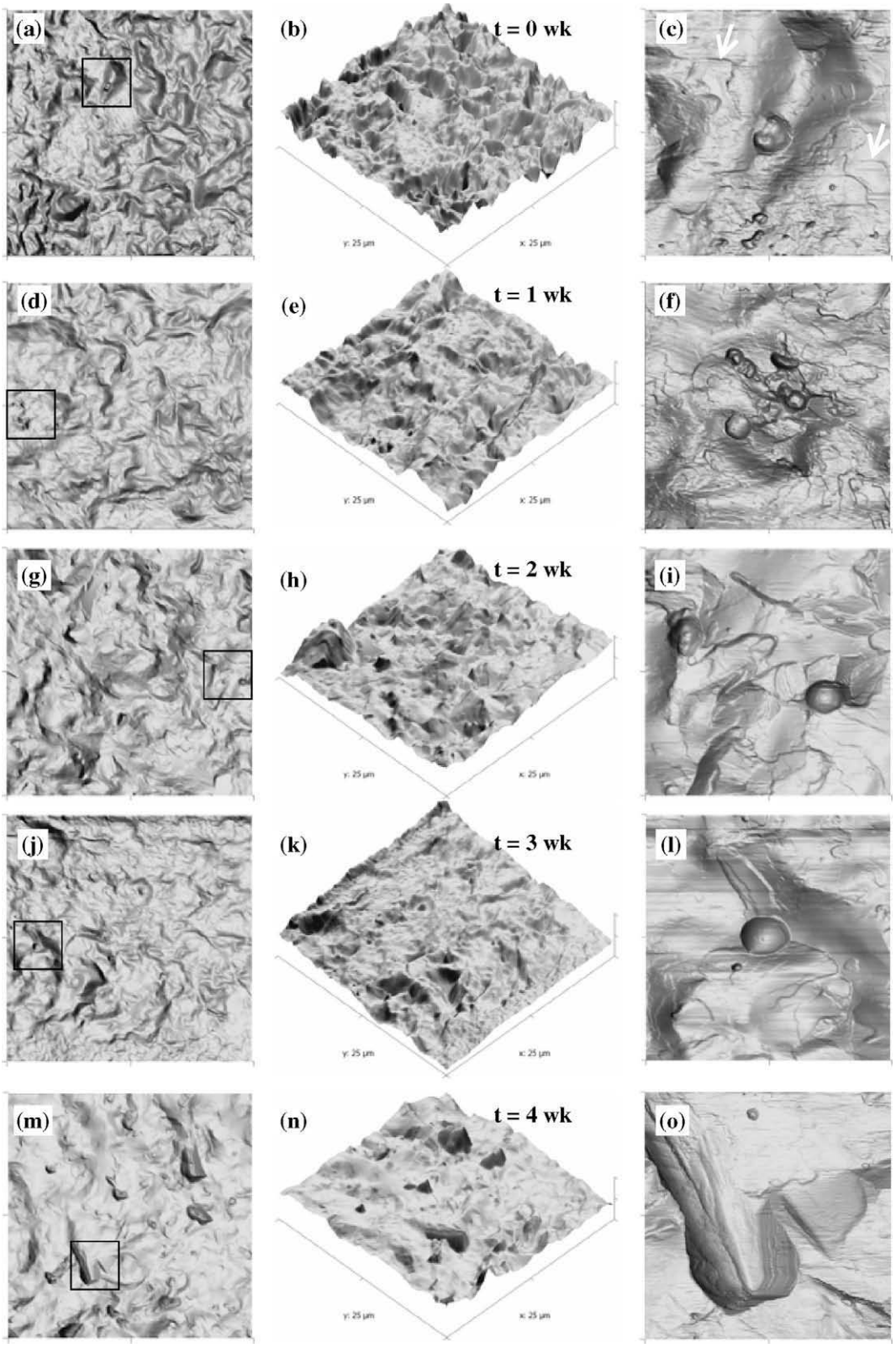

Fig. 3. AFM scans of chocolate #3 repeatedly cycled from 26 to 29 °C over 4 weeks. The left-hand column represents 2-D scans with the corresponding 3-D projections shown in the middle column (25 × 25 μm). The scans in the right-hand column are close-up scans of the area identified by the square boxes in the 25 × 25 μm scans (5 × 5 μm for (c), (f), (i), (l) and (o)). The *z*-axis scale (2 μm per division) is accentuated to better depict areas of interest.

maintained their surface gloss during the entire study. However, addition of 7.5% MF made for a chocolate too soft to handle with a lack of snap and poor melting properties. The addition of 5% MF was a suitable compromise between maintaining the sensory properties of chocolate and robustness to temperature-cycling.

To ascertain the impact of temperature-cycling, chocolate #1 was stored isothermally at 26 ± 0.5 °C for 4 weeks (Fig. 5). AFM re-

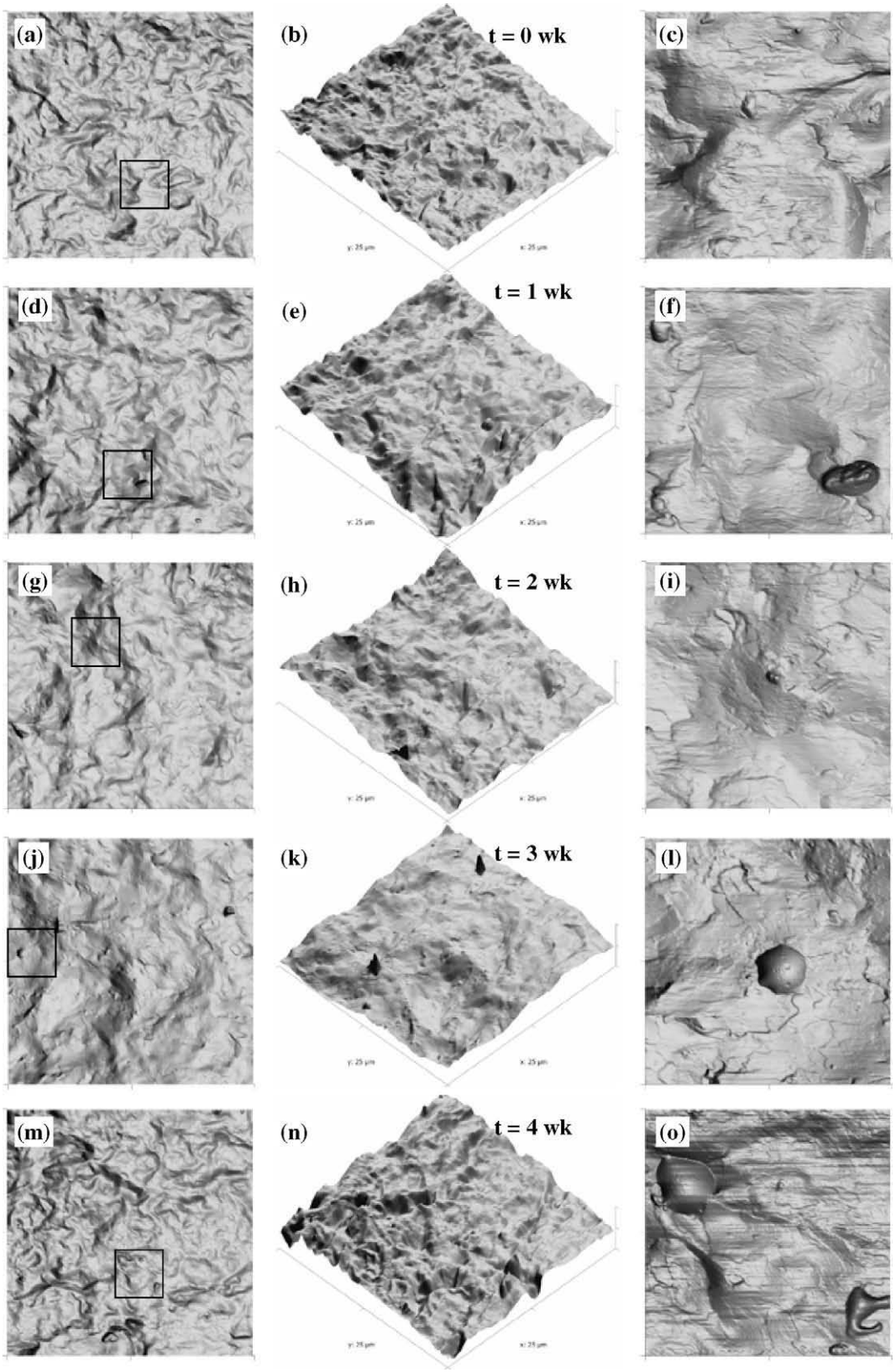

Fig. 4. AFM scans of chocolate #4 repeatedly cycled from 26 to 29 °C over 4 weeks. The left-hand column represents 2-D scans with the corresponding 3-D projections shown in the middle column (25 × 25 μm). The scans in the right-hand column are close-up scans of the area identified by the square boxes in the 25 × 25 μm scans (5 × 5 μm for (c), (f), (i), (l) and (o)). The *z*-axis scale (2 μm per division) is accentuated to better depict areas of interest.

vealed that its microstructural evolution was dominated by changes in cone morphology and crystallisation, and much less by the surface crystallisation seen with temperature-cycling. Images on the first row (Fig. 5a–c) are representative of isother-

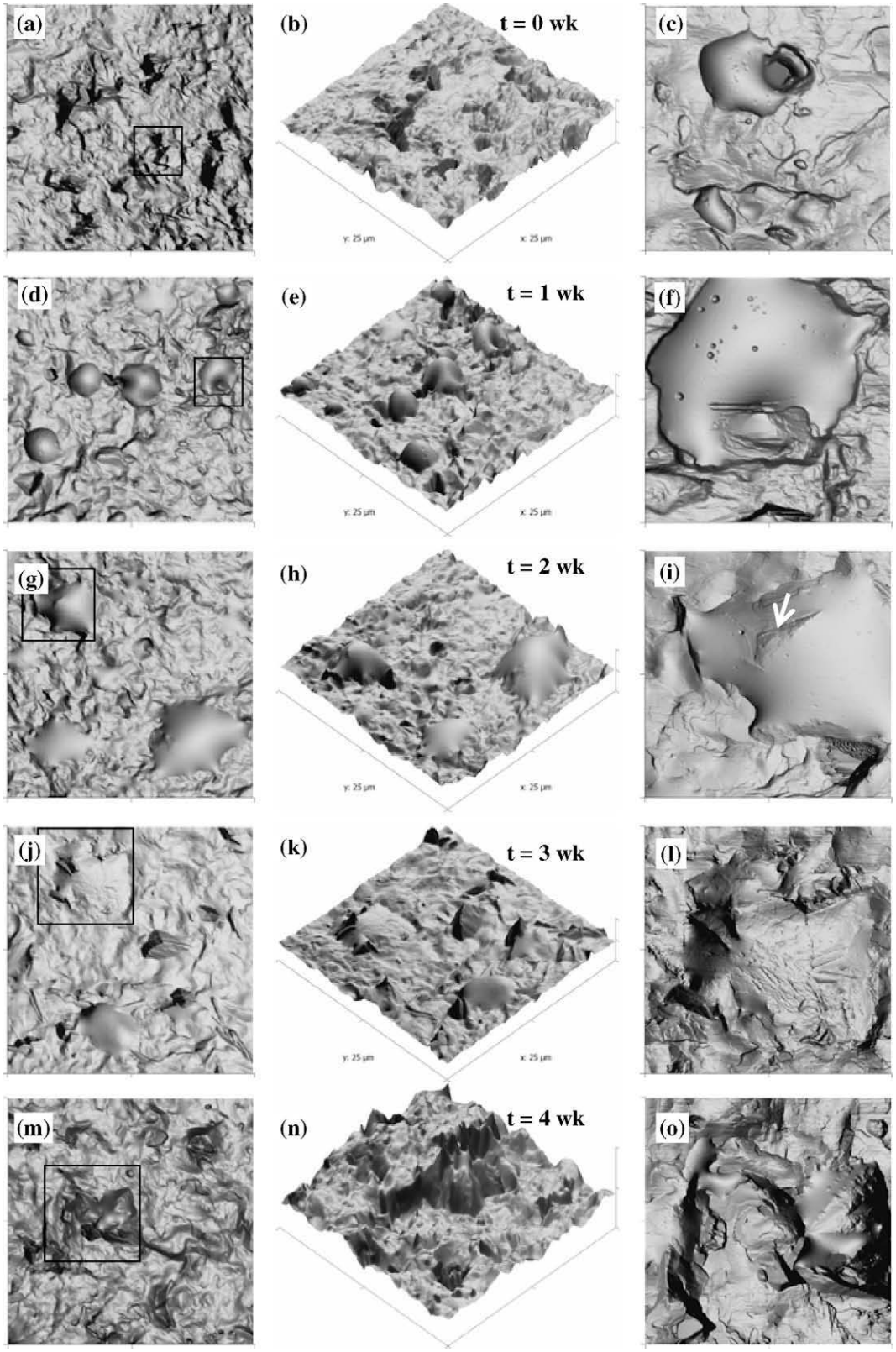

Fig. 5. AFM scans of chocolate #1 stored isothermally at 26 °C over 4 weeks. The left-hand column represents 2-D scans with the corresponding 3-D projections shown in the middle column (25 × 25 μm). The scans in the right-hand column are close-up scans of the area identified by the square boxes in the 25 × 25 μm scans (5 × 5 μm for (c) and (f), 7.5 × 7.5 μm for (i), 10 × 10 μm for (l) and (o)). The *z*-axis scale (2 μm per division) is accentuated to better depict areas of interest.

mally-stored chocolate #1 1 h after demoulding (week 0 sample). Cone texture and concentration were as in its temperature-cycled counterpart (Fig. 1a–c). After 1 week (Fig. 5d–f), more cones were present (average base diameters of ~3.68 ± 0.2 μm), with evidence of surface pitting. By 2 weeks (Fig. 5g–i), there was a continued increase in both cone number and base diameter, with several of

these now appearing 'textured' (arrow in Fig. 5i). By 3 weeks (Fig. 5j–l), the surface of many cones roughened, with numerous protrusions present, indicative of solidification. The remainder of the chocolate surface also exhibited some crystal growth, but much less than with temperature-cycling. Finally, after 4 weeks (Fig. 5m–o), substantial changes in microstructure were apparent, with numerous crystals jutting out vertically from the cones.

AFM was also used to determine changes in surface roughness over time. The RMS roughness of the fresh chocolates ranged from 121 ± 29 nm to 168 ± 9 nm ($p < 0.05$) (Fig. 6), with more MF generally leading to a lower initial roughness. With temperature-cycling, chocolate #1 demonstrated the highest RMS roughness increase over 4 weeks (~165%) whilst chocolate #4 exhibited the smallest (~97%). The RMS roughness of all cycled chocolates increased linearly with time (r^2 = 0.87–0.97) (Fig. 6 and Table 1), with slower changes in roughness [i.e., a decreasing slope (ΔRMS/week)] as a function of MF content. This was consistent with the reduced crystal growth observed in Figs. 1–4. The RMS roughness of the isothermally-stored chocolate #1 increased ~98% over 4 weeks, which was lower than the RMS evolution of cycled chocolates #1–#3 and similar to chocolate #4. This not only emphasised the dramatic influence of temperature-cycling on topography, but also confirmed that the surface crystals formed through cycling contributed more to surface roughening than did the cones.

3.3. Polymorphic transitions during storage

All samples were initially in form V polymorph with a very strong diffraction peak at 4.58 Å and four smaller peaks at 3.99, 3.87, 3.75 and 3.68 Å (Fig. 7). Small-angle XRD results indicated two key long spacings at 63.0 and 32.1 Å (data not shown), typical of CB's form V (Wille & Lutton, 1966). There was a gradual transition towards form VI in all samples, though at different rates (Fig. 8). Cycled chocolate #1 exhibited the fastest rate of form VI development and at 4 weeks had completely transformed into form VI, with a very strong diffraction peak at 4.58 Å and three smaller trademark peaks at 4.04, 3.86 and 3.70 Å (Wille & Lutton, 1966) (Fig. 7a). Partial replacement of CB with MF slowed this transition with the 2.5% and 5% MF chocolates having similar spectra after 4 weeks (Fig. 7b and c). The presence of 7.5% MF nearly halted the form V → VI transition (Fig. 7d). The polymorphic evolution of isothermally-stored chocolate #1 (Fig. 7e) was slowest, with the form V → VI phase transition only starting at 2 weeks. By 4 weeks,

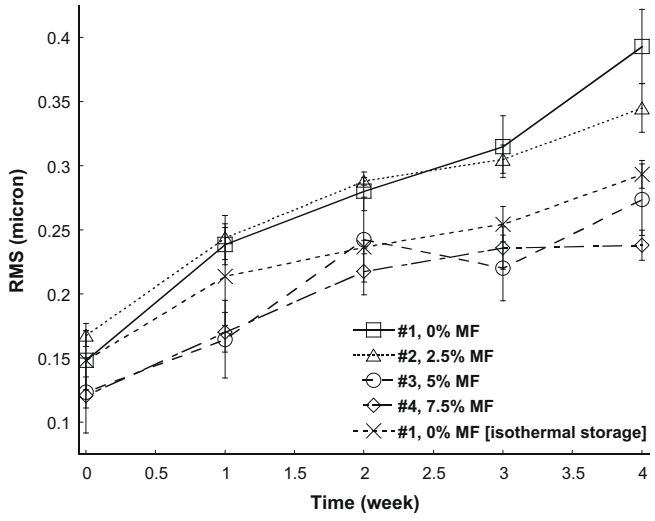

Fig. 6. Evolution in surface (RMS) roughness in temperature-cycled chocolates #1–#4 and isothermally-stored chocolate #1 with storage time.

Table 1
Change in RMS surface roughness over 4 weeks of temperature-cycling from 26 to 29 °C and in isothermally-stored chocolate #1.

Chocolate	ΔRMS/week (nm)	r^2
#1	57	0.97
#2	42	0.94
#3	36	0.87
#4	30	0.89
#1 (isothermal)	33	0.94

the proportions of form VI were ~50%, ~35% and ~20% for temperature-cycled chocolates #2–#4, respectively, whereas the proportion of form VI in the isothermally-stored chocolate was ~10%.

Besides the evident polymorphic transition, evolution in the diffraction peaks indicated that crystal perfecting was taking place with time as the key Bragg peaks for all samples sharpened, particularly with repeated temperature-cycling. For example, after 4 weeks, the form VI peaks in temperature-cycled chocolate #1 were sharper than at any other time point. Similarly, in chocolate #4, well-defined peaks predominantly associated with form V were much sharper than at week 0. Such crystal annealing, which has been observed in other polycrystalline materials, such as pharmaceutical drugs (Kim, Wei, & Kiang, 2003), metals (Wang, Pavlidis, & Cao, 1997) and proteins (Juers & Matthews, 2004), is indicative of increased uniformity in crystal orientation, crystal size, and/or lessened variability in unit cell distances. With repeated temperature-cycling, there was also increased mass transfer, and thus possible TGs fractionation taking place. This would lead to further annealing, resulting in accelerated crystal growth and promotion of the polymorphic transition to form VI, compared with isothermal storage.

3.4. Changes in solid fat content with time

At week 0, SFCs ranged from 81.0 ± 0.2% for chocolate #1 to 72.5 ± 0.2% for chocolate #4 (Fig. 9). The reduction in initial SFC was probably a combination of 3 factors: (i) MF's inherent lower SFC than that of CB between 26 and 29 °C; (ii) partial CB solubilisation in MF, particularly at 29 °C; and (iii) the possibility of a eutectic effect arising from the CB–MF mixture (Hartel, 1996). The SFC of all chocolates decreased during the first 1–2 weeks of cycling and reached SFC_{min} before gradually increasing, though this depended on MF content. The maximum reduction in SFC [(SFC at $t = 0$) − (SFC_{min})] were ca. 1.0%, 3.4%, 4.6% and 5.1% for chocolates #1–#4, respectively, whereas those from weeks 0 to 4 were ca. +1.6%, −3.2%, −5.0% and −5.8%. The SFC drop during the first 1–2 weeks strictly resulted from the repeated temperature changes as the SFC of the isothermally-stored control increased 3.6% over 4 weeks, with no decrease observed. After 4 weeks, this chocolate tended towards a plateau SFC of ~84.0 ± 0.1%.

The decrease in SFC with cycling may be explained by the de-tempering of the fat phase and its uncontrolled re-crystallisation, with the presence of MF playing a key role. The chocolate was initially tempered at ~15 °C, yielding SFCs of 72.5–81.0% at 26 °C at week 0 and the dominance of form V crystals. With heating to 29 °C for 12 h, smaller form V crystals melted, given either their higher solubility *vis-à-vis* larger crystals and/or constituent TGs having a lower-melting point – e.g., if CB crystals consisted of POS and POP vs. SOS, they likely melted at a lower temperature (Arishima, Sagi, Mori, & Sato, 1991). Upon cooling to 26 °C, only some of the melted fat re-crystallised – this process being uncontrolled and at a higher temperature than that during the initial tempering. Thus, the resulting SFC was not as high as the first time point. Repeated cycling led to SFC_{min}, after which SFCs either reached a plateau or started to increase. Speculatively, SFC_{min} corresponded to an equilibrium SFC under this set of cycling con-

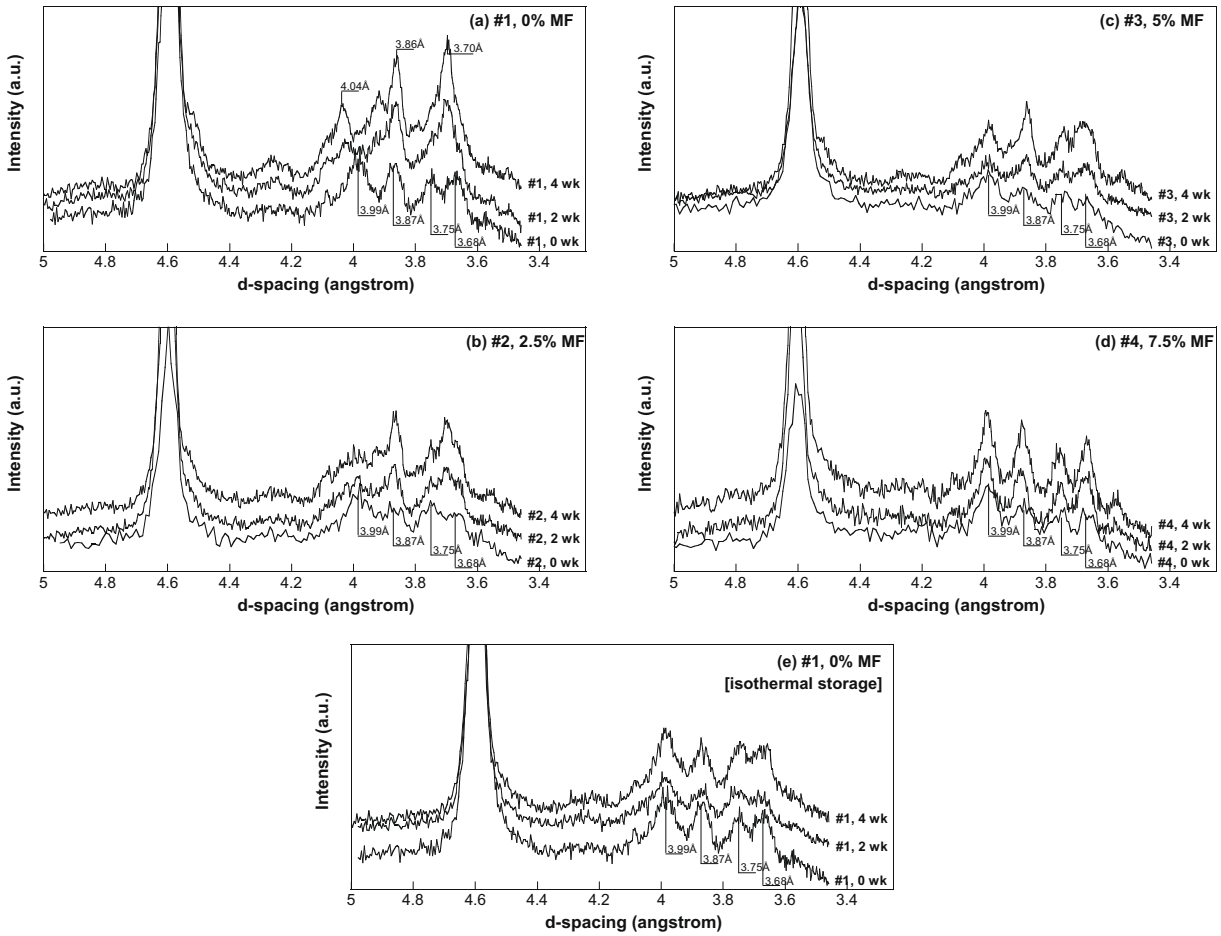

Fig. 7. Evolution in X-ray diffraction patterns in temperature-cycled chocolates #1–#4 and isothermally-stored chocolate #1 with storage time.

ditions. Had other setpoints or a different temperature gradient been used, different SFC_{min} values would have resulted. In parallel, there was evolution in fat phase polymorphism, though a correlation between SFC and XRD was not readily apparent, as the form V → VI increase was relatively linear whereas the change in SFC was not.

With cycling, only part of the melted fat re-crystallised, either into larger form V crystals or newly-formed form VI crystals *via* melt-mediated templating of pre-existing crystals, thus resulting in an increased average crystal size on the chocolate surface. This occurred with all samples, though it was particularly evident for chocolate #2 (2.5% added MF). Contrary to convention, lower SFCs

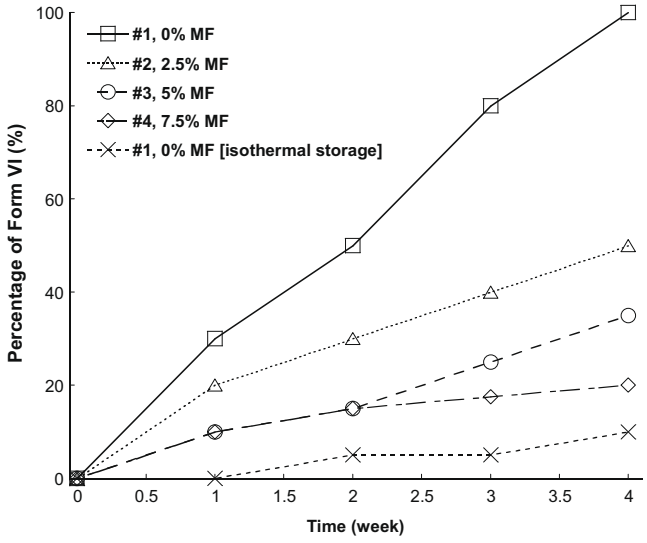

Fig. 8. Proportion of form VI in temperature-cycled chocolates #1–#4 and isothermally-stored chocolate #1 with storage time.

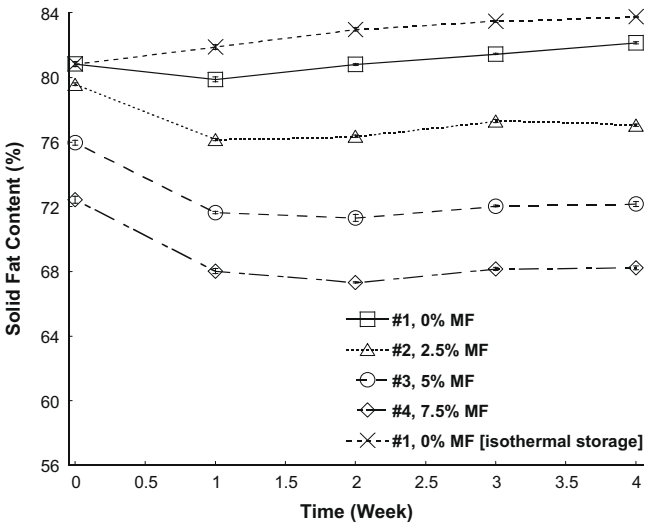

Fig. 9. Evolution in solid fat content in temperature-cycled chocolates #1–#4 and isothermally-stored chocolate #1 with storage time.

did not accelerate the form V → VI transition. For example, when a hard fat (e.g., a fully hydrogenated vegetable oil) is mixed with liquid oil, the β' to β transition will usually be accelerated, with this ascribed to the greater conformational freedom of the higher-melting TGs to adopt their most favourable configuration. Though resulting in lower SFCs, MF hindered CB's polymorphic transformation (Timms, 2003), probably as a result of TGs in MF's high melting fraction co-crystallising with CB TGs to form mixed-species unit cells. In chocolate #1, given the absence of MF, there was no such restriction, and the fat phase readily transformed into form VI.

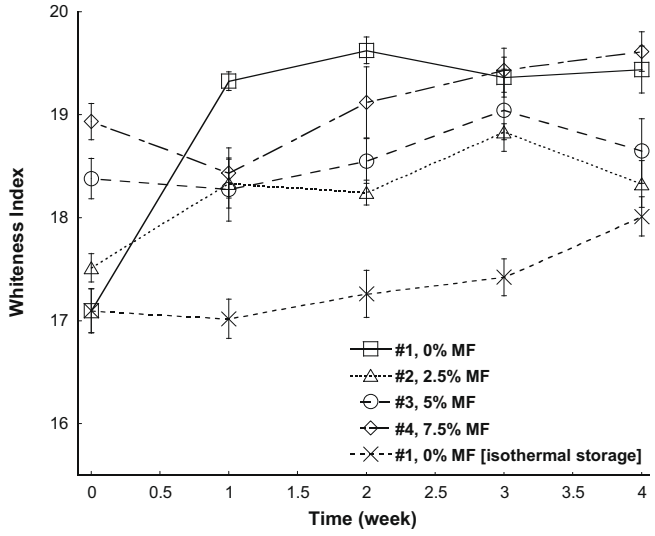

Fig. 10. Evolution in whiteness index in temperature-cycled chocolates #1–#4 and isothermally-stored chocolate #1 with storage time.

3.5. Surface whiteness index (WI)

Chocolate #1 had the lowest WI amongst all treatments, given its MF-free formula (Fig. 10). However, its WI increased the most over 4 weeks ($p < 0.05$), due to the extensive development of surface crystals (Fig. 1). Changes in WI over 4 weeks for chocolates with 2.5–7.5% MF were not significantly different ($p > 0.05$). The changes in relative WI from weeks 0 to 4 were ca. +2.34, +0.81, +0.27 and +0.68 for chocolates #1 through #4, respectively. The change in the WI of isothermally-stored chocolate #1 over 4 weeks was +0.91 which, given the relative lack of surface crystallisation discussed earlier, resulted from cone-related crystallisation (Fig. 5). By the end of the study, only cycled chocolates #1 and #2 appeared slightly visually bloomed with chocolates #3 and #4 retaining their original surface gloss. In the case of isothermally-stored chocolate #1, no visual bloom was detected.

3.6. Role of MF on microstructural evolution

The distinction between surface crystallisation and cone evolution depended on fat phase composition and storage conditions, as other key parameters (tempering, other ingredients) were kept constant. With different amounts of MF, fresh chocolate topography was distinguished by the presence and properties of the welled cones, with no differences in CB surface crystals. *Sans* MF, chocolate #1 had a higher SFC and was likely subjected to greater contraction, leading to more extensive welling of liquid fat to the surface and the formation of larger deposits (Figs. 1 and 5). With 2.5% MF, the lower SFC likely reduced contraction, leading to fewer, smaller drops at the surface (Fig. 2). In chocolates #3 and #4, the initial SFC was even lower, which hinted at reduced contraction and thus fewer, if any, surface deposits (Figs. 3 and 4). Rather, on these latter chocolates, there existed smooth, flat regions on the surface that, speculatively, consisted of lower-melting fat that

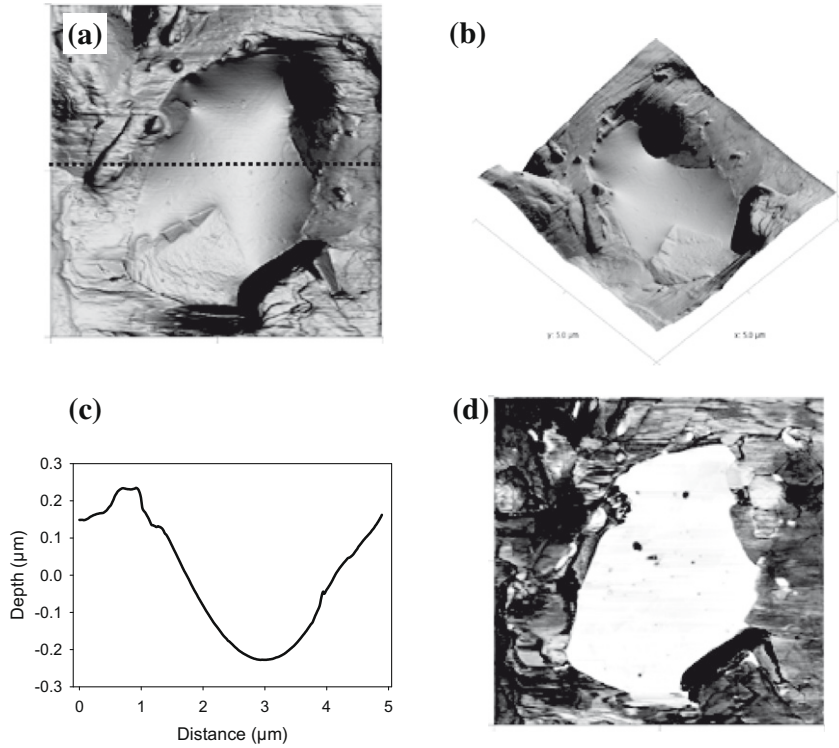

Fig. 11. The presence of smooth, flat regions on the surface of chocolate #3 that may demonstrate cone formation in progress. Figure (a) is a 2-D image whereas (b) is the equivalent 3-D representation. Image (c) is a cross-sectional profile of the dotted line across (a). Image (d) is the corresponding phase image showing rheological dissimilarity between the central portion of the image and its surroundings.

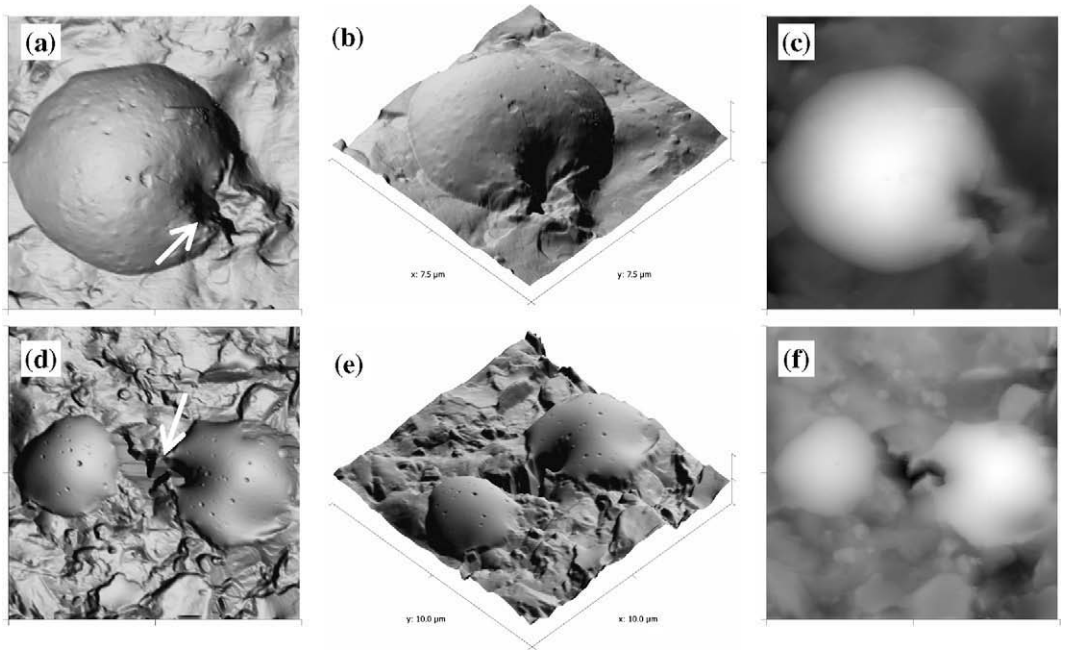

Fig. 12. AFM scans of chocolate #1 at week 0 (isothermal) (a–c) and at week 1 (isothermal) (d–f) showing the proximity between welled regions and surface pits (white arrows). Images (a) and (d) are 2-D scans with the corresponding 3-D projections in the middle column [(b) and (e)]. The right column shows the related topographic presentation [(c) and (f)]. The top row images are 7.5 × 7.5 μm in size whereas images on the bottom row are 10 × 10 μm in size. The *z*-axis scale is 2 μm per division.

had not completely welled to the surface (Fig. 11), either due to insufficient contraction or perhaps the unavailability of molten fat. Fig. 11a and b shows a 2-D and 3-D view of such a region ~3 × 4 μm in size, with Fig. 11c showing the cross-sectional profile of the line in Fig. 11a. The phase scan (Fig. 11d) distinguishes the softer (bright) region from the surrounding harder matrix, confirming the dissimilar SFC or composition of the fat in the central region compared to its surroundings.

Height images of chocolate #1 (Fig. 12) show the presence of surface depressions surrounded by well-defined cones. Both series of images (Fig. 12a–c and 12d–f show openings that appear to be the source of expelled lower-melting fat, possibly responsible for surface deposition. Fig. 12a–c shows a single cone in close proximity to a pit (white arrow). In Fig. 12d–f, the scan of a 'double' cone shows an irregularly-shaped pit, ~1.5 μm in depth, nestled between two cones (white arrow). In contrast to our earlier work (Sonwai & Rousseau, 2008), where cones formed on the surface of milk chocolate, with and without Coberine (a CBE), were very smooth, many of the cones here exhibited pitting, in particular on chocolate #1 (no added MF). It is possible that these pits were nucleation sites for higher-melting TGs (Sonwai & Rousseau, 2008). Addition of MF led to reduced cone formation and reduced pitting, a probable consequence of the lower SFC and increased CB TG solubilisation.

4. Conclusion

Post-processing fat (re-)crystallisation in chocolate is a complex phenomenon, in part driven by composition and storage conditions. The presence of MF is beneficial in preventing fat bloom, but only beyond a critical concentration, >2.5% of the finished product. Below this level, MF still slows the form V → VI transition, but appears to increase surface crystal growth when chocolates are subjected to cycling. The addition of 5% MF is a suitable compromise between maintaining the sensory properties of chocolate and robustness to temperature-cycling.

This study also demonstrates that 2 crystallisation phenomena concurrently take place in chocolate: (i) the growth of pre-existing surface crystals that act as templates for larger bloom-causing crystals and (ii) amorphous, welled regions ('cones') that solidify with age and act as loci for crystal outcrops. The latter dominates under constant temperature conditions whereas surface crystallisation dominates with temperature fluctuations. Temperature-cycling accelerates the growth of existing surface crystals through repeated partial melting and solidification of the fat phase, with liquid-state TGs promoting the growth of existing platelet crystals, probably *via* a templating effect. In parallel, crystal growth appears slower on the cones than on the background surface. It is feasible that TG make-up of the cones differs from the rest of the chocolate, which would help to explain their presence.

When viewed from an industrial, post-consumer purchase viewpoint, it is best to think of microstructural evolution and fat crystallisation in chocolate as a combination of both fluctuating and isothermal storage, where surface crystallisation and cone solidification occur concurrently.

Acknowledgements

Nigel Sanders of Cadbury Canada (Toronto, Canada) is thanked for the preparation of the chocolate samples. Funding from the Natural Sciences and Engineering Research Council of Canada (NSERC), from a Premier's Research Excellent Award from the province of Ontario, Canada, and from Ryerson University, is also acknowledged.

References

Aguilera, J. M., Michel, M., & Mayor, G. (2004). Fat migration in chocolate: Diffusion or capillary flow in a particulate solid? – A hypothesis paper. *Journal of Food Science, 69*(7), R167–R174.

Arishima, T., Sagi, N., Mori, H., & Sato, K. (1991). Polymorphism of POS. I. Occurrence and polymorphic transformation. *Journal of the American Oil Chemists Society, 68*(10), 710–715.

Hartel, R. (1996). Applications of milk-fat fractions in confectionery products. *Journal of the American Oil Chemists Society, 73*(8), 945–953.

Jewell, G. (1972). Some observations on bloom on chocolate. *International Chocolate Review, 27*, 161–162.
Juers, D. H., & Matthews, B. W. (2004). The role of solvent transport in cryo-annealing of macromolecular crystals. *Acta Crystallographica Section D: Biological Crystallography, 60*(3), 412–421.
Kim, S., Wei, C., & Kiang, S. (2003). Crystallization process development of an active pharmaceutical ingredient and particle engineering via the use of ultrasonics and temperature-cycling. *Organic Process Research and Development, 7*(6), 997–1001.
Lohman, M. H., & Hartel, R. W. (1994). Effect of milk fat fractions on fat bloom in dark chocolate. *Journal of the American Oil Chemists Society, 71*(3), 267–276.
Loisel, C., Keller, G., Lecq, G., Bourgaux, C., & Ollivon, M. (1998). Phase transitions and polymorphism of cocoa butter. *Journal of the American Oil Chemists Society, 75*, 425–439.
Lonchampt, P., & Hartel, R. W. (2004). Fat bloom in chocolate and compound coatings. *European Journal of Lipid Science and Technology, 106*, 241–274.
Rousseau, D., & Smith, P. R. (2008). Microstructure of fat bloom development in plain and filled chocolate confections. *Soft Matter, 4*(8), 1706–1712.
Rousseau, D., & Sonwai, S. (2008). Influence of the dispersed particulate in chocolate on cocoa butter microstructure and fat crystal growth during storage. *Food Biophysics, 3*, 273–278.
Sonwai, S., & Rousseau, D. (2006). Structure evolution and bloom formation in tempered cocoa butter during long-term storage. *European Journal of Lipid Science and Technology, 108*, 735–745.
Sonwai, S., & Rousseau, D. (2008). Fat crystal growth and microstructural evolution in industrial milk chocolate. *Crystal Growth and Design, 8*(9), 3165–3174.
Timms, R. E. (1984). Phase behaviour of fats and their mixtures. *Progress in Lipid Research, 23*(1), 1–38.
Timms, R. E. (2003). *Confectionery fat handbook – Properties. Production and applications*. London: The Oily Press.
Vaeck, S. (1960). Cocoa butter and fat bloom. *The Manufacturing Confectioner, 40*(6), 35–74.
Wang, K., Pavlidis, D., & Cao, J. (1997). Effect of in situ thermal cycle annealing on GaN film properties grown on (0 0 1) and (1 1 1) GaAs, and sapphire substrates. *Journal of Electronic Materials, 26*(1), 1–6.
Wille, R. L., & Lutton, E. S. (1966). Polymorphism of cocoa butter. *Journal of the American Oil Chemists Society, 43*(8), 491–496.